Photon counting linear mode global shutter flash LIDAR for improved range performance

Lane Fuller, Amy Carl, Joe Spagnolia, Brad Short, Michael Dahlin
Advanced Scientific Concepts, LLC
125 Cremona Drive, Suite 250, Goleta, CA 93117

ABSTRACT

Linear mode global shutter flash LIDAR (gsf-LIDAR) is addressing the need for 3D sensing in a wide range of space, airborne, autonomous vehicle, and marine applications. Flash LIDAR produces real time dense 3D point clouds, enriched with scene intensity information, that are not subject to motion distortion. Current and future applications require extended range performance from a low Size Weight and Power (SWaP) 3D sensor. A Linear Mode LIDAR with photon sensitivity comparable to Geiger Mode sensing is needed to meet the challenges. Geiger mode APDs sensors require high repetition rate lasers to allow multiple frame summing and the associated processing overhead creates a significant SWaP burden. Advanced Scientific Concepts LLC has developed a linear mode gsf-LIDAR camera which has significant improvements in the minimum photon detection threshold, 10X for a single frame and over 30X with the aid of frame summing, which offers long range performance with low flux photon counting capability. ASC 3D Flash LIDAR uncooled testing demonstrated sub 30 photon detection with a low repetition rate laser. This performance improvement enables low SWaP sensors for enhanced space-based LIDAR capabilities for rendezvous /docking and planetary landing hazard detection and avoidance applications.

Keywords: Linear Mode Global Shutter Flash LIDAR, Photon Counting, 3D Mapping, Object Detection and Tracking, Proximal Satellite Operations, Landing Hazard Detection and Avoidance

1. INTRODUCTION

LIDAR systems are an emerging technology with a variety of modalities: Scanning, Phase Modulated, Geiger Mode, Flash, etc. ASC's LIDAR is unique in that it implements a "global shutter" which captures a full frame of range and intensity data with a single laser pulse. Each frame is analogous to a 2D camera snapshot with the addition of range information provided for each pixel. The global shutter flash LIDAR (GSFL) does this by emitting a short (6-10ns) laser pulse that is spread by a diffuser to illuminate the entire field of view (FOV). Using ASC's patented readout technology, each pixel samples this single laser pulse 20 times and sends these samples along with the associated time of flight (ToF) to a field programmable gate array (FPGA) to be converted to range and intensity values. As a result, the GSFL produces an organized 3D point cloud of a scene that is essentially frozen in time and free of motion blur without the need for any post processing. This is essential for guidance, navigation, and control (GNC) and real-time 3D mapping applications and cannot be achieved with LIDAR that build images sequentially with high repetition rate lasers without significant processing and SWaP overhead. Despite these SWaP and processing disadvantages, Geiger Mode LIDAR are often preferred due to their higher photon sensitivity and extended range performance.

With its latest GSFL design, ASC has addressed this sensitivity disparity with Geiger Mode LIDAR while maintaining the real-time advantages inherent in Flash LIDAR. This design utilizes a focal plane array (FPA) of 128x128 linear mode indium gallium arsenide (InGaAs) avalanche photodiode (APD) detectors and low noise readout capable of gated-mode operation [1][2]. A commonly cited threshold for detection for Flash LIDAR is 1000 photons [3]. The test presented in this paper demonstrates 10X improvement on this threshold and a 30X improvement with the aid of frame summing. In order to verify sensitivity improvements, ASC designed and performed a precise radiometric test using a modified GSFL testbed which was uncooled and operating at room temperature. This paper discusses this test in detail and analyzes the resultant performance of the FPA. Finally, implications for current and future applications are discussed.

2. METHODOLOGY

2.1 Optical design

ASC developed an experiment to demonstrate GSFL sensitivity by focusing a known amount of input light onto the FPA and measuring the output. A block diagram of the test setup is shown in Figure 1, a photo is shown in Figure 2, and an equipment list is shown in Table 1. In order to measure the input light, a fiber coupled laser diode was split into two branches using a 90:10 fiber splitter. The 90% end of the splitter was directed into a high sensitivity energy meter, and the 10% end was directed onto the GSFL FPA. The 10% splitter output was collimated and focused down to a spot size less than the active area of a single APD detector. Focusing all the light onto a single pixel simplifies the analysis as the relative distribution over many pixels does not need to be considered. Linear stages in the x, y, and z directions were used to center the spot on a pixel and ensure the FPA is located at the focus of the lens. APD detectors on the GSFL are much more sensitive than off-the-shelf energy meters so calibrated neutral density (ND) filters were used to reduce the amount of input light. A large number of ND filters would be needed to sweep the full dynamic range of the GSFL, so a variable fiber attenuator was also inserted into the optical path. This allowed for much finer steps between each ND filter. At each attenuation setting, 100 frames of raw GSFL data along with the corresponding measurements from the energy meter were collected.

2.2 Temporal signal chain

The normal mode of operation for the GSFL is to send out a laser pulse and measure the time it takes for the reflected pulse to return to the FPA. A pulse generator along with a testbed version of the GSFL were used to simulate the time delay of an object at range while maintaining the test setup described above. The mode of operation was adjusted to the following: the GSFL outputs a signal to fire the laser, energizes the FPA, and starts the counters. Then, the laser fire signal was fed into the external trigger of the pulse generator which waits a fixed delay before producing an 8ns square pulse to drive the laser diode. The time delay of the pulse generator is user programmable so any range can be simulated, but this was kept fixed for this test. Therefore, each frame the GSFL measured a return pulse at the same time delay (i.e., the same range). The GENTEC energy meter is equipped with an internal digital trigger and did not need to be triggered externally.

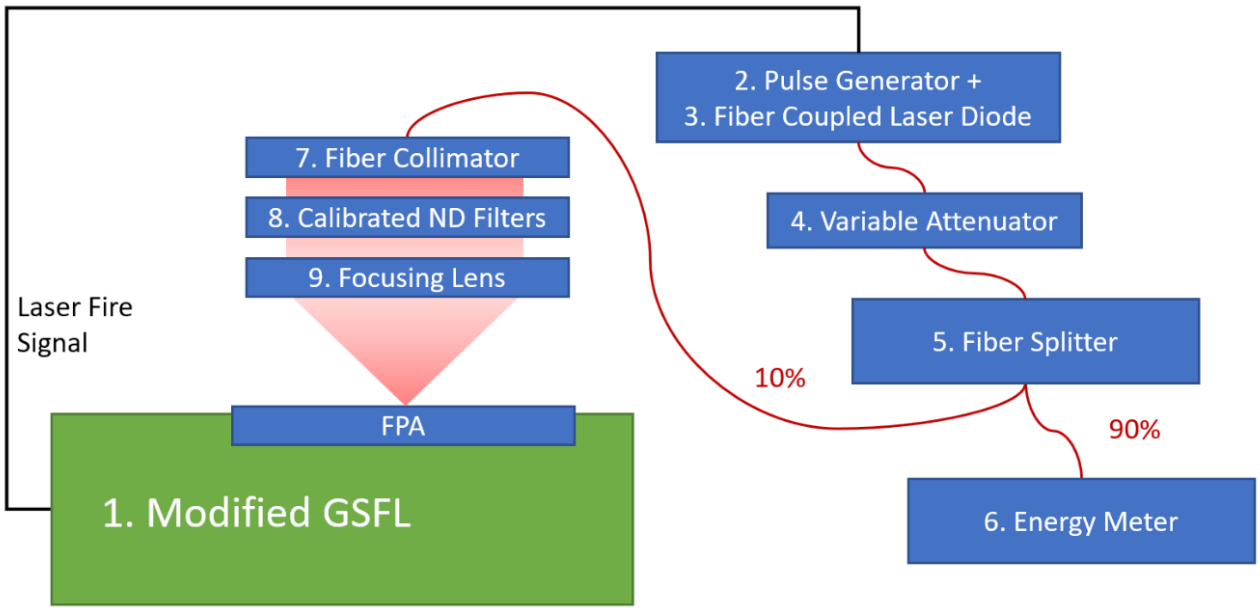

Figure 1: Test setup block diagram

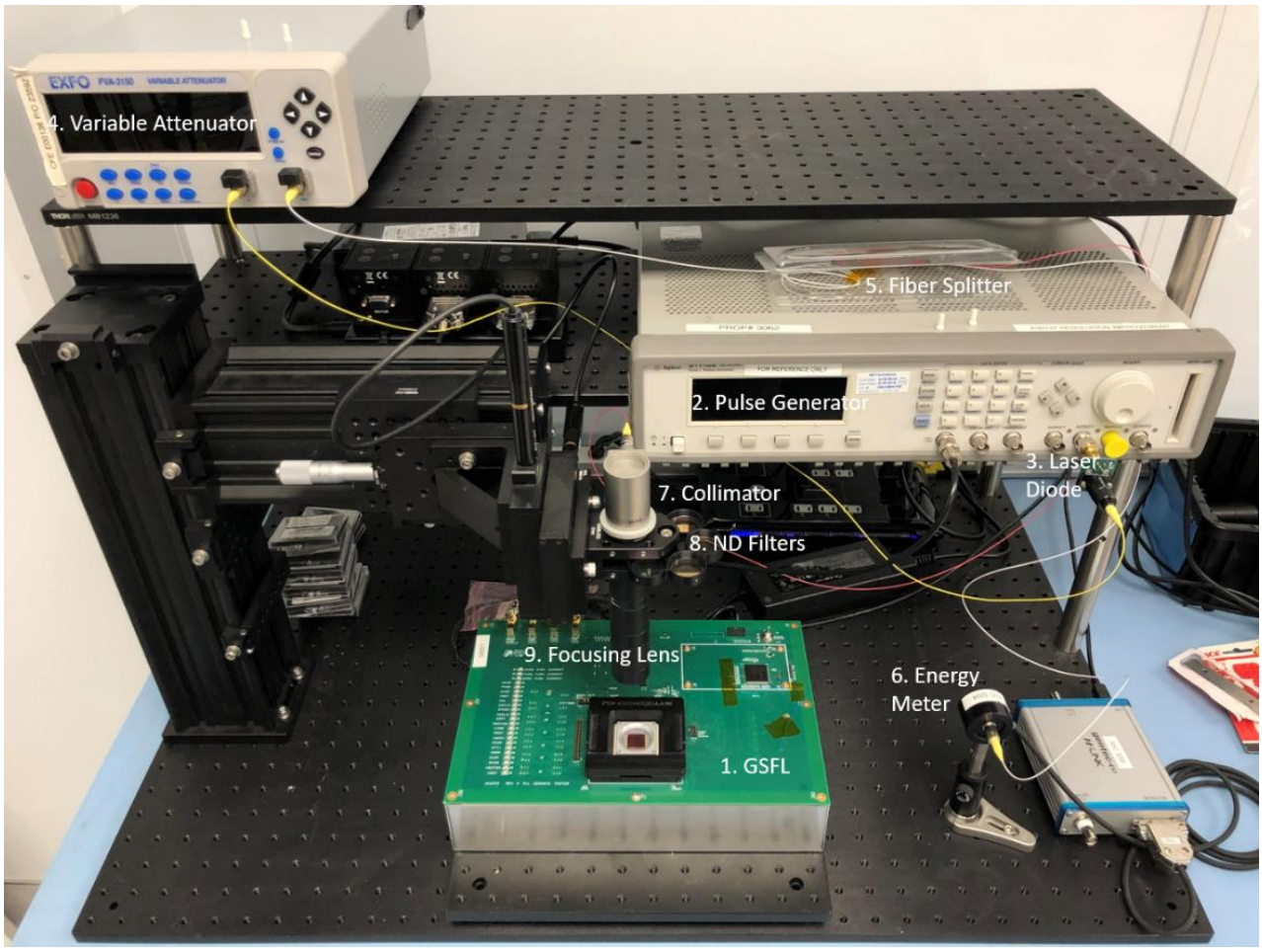

Figure 2: Test setup image

Table 1: Equipment list

Item #	Description	Manufacturer	Part #
1.	GSFL Testbed	ASC	N/A
2.	Pulse Generator	Keysight	81110A
3.	SM Fiber-Pigtailed Laser Diode	Thorlabs	LPS-1060-FC
4.	Variable Attenuator	EXFO	FVA-3150
5.	90:10 Fiber Splitter	Thorlabs	TW1064R2F1B
6.	Laser Energy Meter	GENTEC-EO	PE3B-Si-D0
7.	Reflective Collimator	Thorlabs	RC12FC-P01
8.	Calibrated ND Filters	Thorlabs	NENIR(05-40)A-C
9.	AR Coated Spherical Lens	Thorlabs	LB254-150-C

3. RESULTS AND ANALYSIS

3.1 GSFL response characterization

The goal of this experiment was to quantify the relationship between the power (or number of photons) of incident light to the output of the GSFL. The GSFL reports both range and grayscale intensity data for each pixel every frame. In order to calculate range and intensity, each GSFL pixel contains a timer and 20-cell buffer that samples the output of the detector. This buffer contains digitized samples of the return pulse and is sent to the FPGA for further processing. The FPGA applies a digital filter to the 20-cell buffer to calculate range to a resolution that is better than the clock sample frequency, and finds the peak of the 20-cell buffer, which is output as the intensity. This intensity value does not have physical units and is simply a 12-bit grayscale taking values from 0-4095. For each laser pulse, both the 20-cell buffer (and corresponding intensity value) along with the energy measurements made by the GENTEC meter were collected. Equation 1 was used to convert from energy at the meter to number of photons incident on the GSFL pixel

$$N_\gamma = \frac{E_m \lambda}{hc} \cdot \eta_{spl} \cdot \eta_{opt} \cdot \eta_{ND} \tag{1}$$

where N_γ is the number of photons incident on the pixel, E_m is the energy measured by the energy meter, λ is the laser diode wavelength, h is Planck's constant, c is the speed of light, η_{spl} is the ratio of the fiber splitter, η_{opt} is the combined transmission of the optics (collimator and lens), and η_{ND} is the transmission of the calibrated ND filter.

The overall results of the test are shown in Figure 3 where each plotted point corresponds to a single laser pulse; the x value of each point is the output of Equation 1 and the y value is the intensity or peak of the 20-cell buffer as described above. This shows that the FPA response is nonlinear at high levels of photon flux. However, the response transitions to a linear regime as the photon flux is decreased below 1000 photons. This is shown on the right side of Figure 3, which is the same data with different limits and a linear regression.

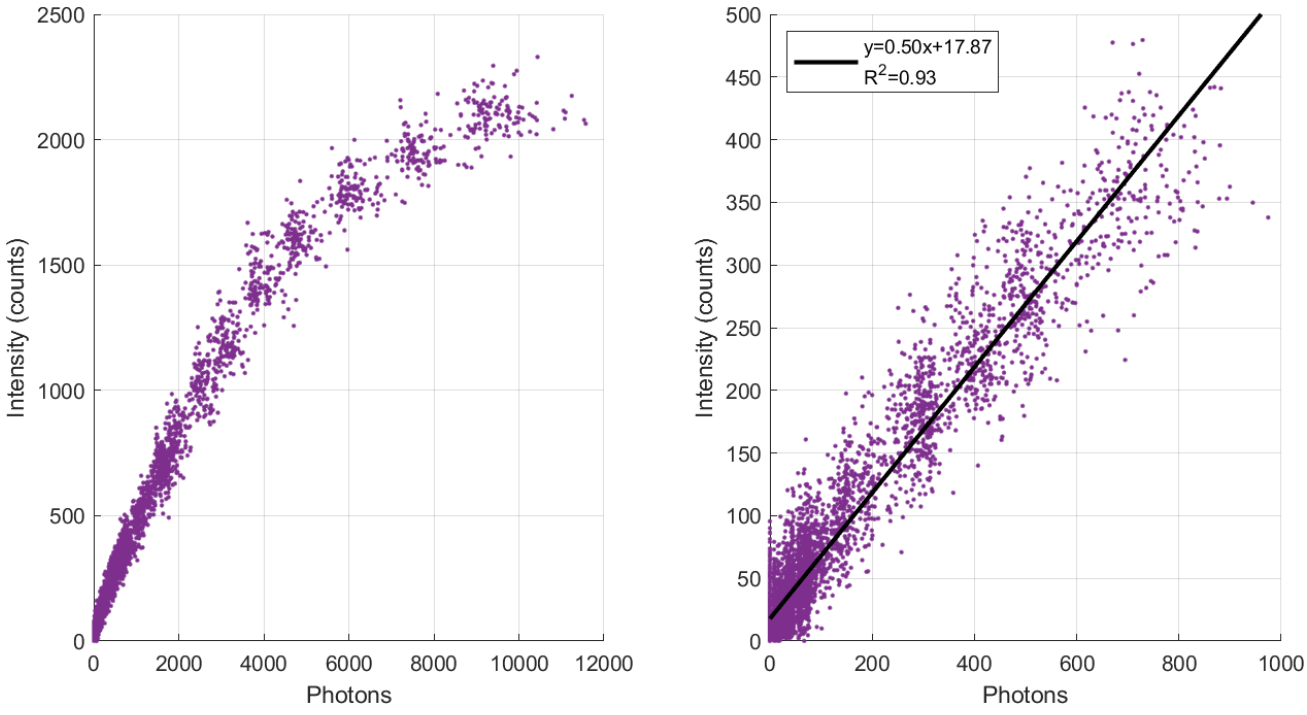

Figure 3: (Left) Relationship between photons incident on a pixel and GSFL intensity. Each cluster corresponds to a distinct attenuation setting. (Right) Same data set zoomed into the linear regime.

3.2 Low photon flux performance

Figure 4 shows the performance of the GSFL with low photon flux. A centroid for each cluster is plotted to show mean photon flux and serve as a key for following plots. In order to demonstrate performance, a simple pulse detection algorithm was developed which consists of a matched filter and a threshold. A matched filter using a typical return pulse shape as a template is applied to the raw 20-cell data collected each frame and at each attenuation level. Then, the peak value of the matched filter output is compared to a threshold value to determine if the return pulse is valid. This algorithm is applied to each cluster shown in Figure 4 and to data collected with the laser off in order to calculate a probability of detection (PD) and probability of false detection (PFD), respectively. Figure 5 shows the PD of the algorithm at five different threshold levels and corresponding PFDs. Not surprisingly, the PD increases as the PFD increases; requirements for each parameter are application-specific so a variety are shown. Regardless of the acceptable PFD, this shows that a 100-photon pulse will be detected at least 80% of the time, which is a significant improvement over the previous 1000-photon threshold.

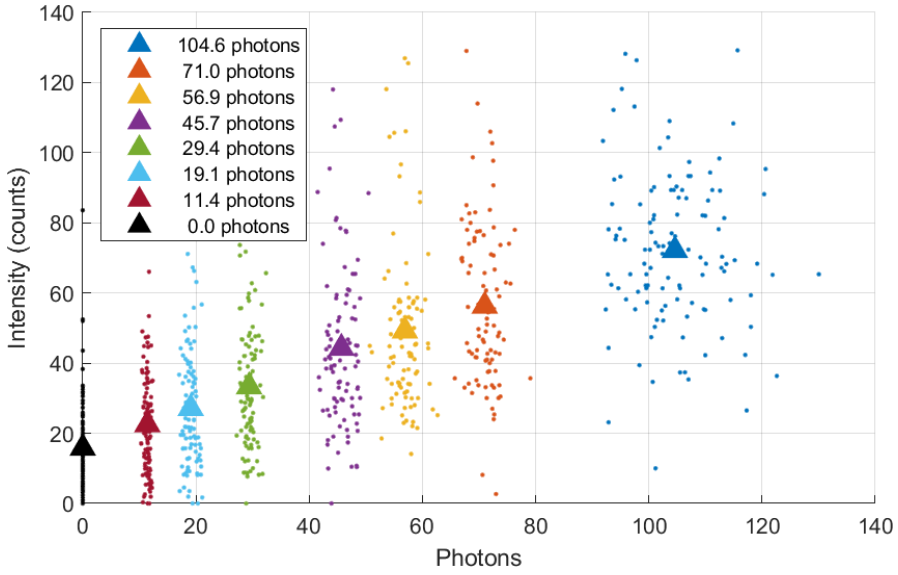

Figure 4: GSFL intensity performance for low photon flux. Centroids show mean intensity and photon flux for each cluster.

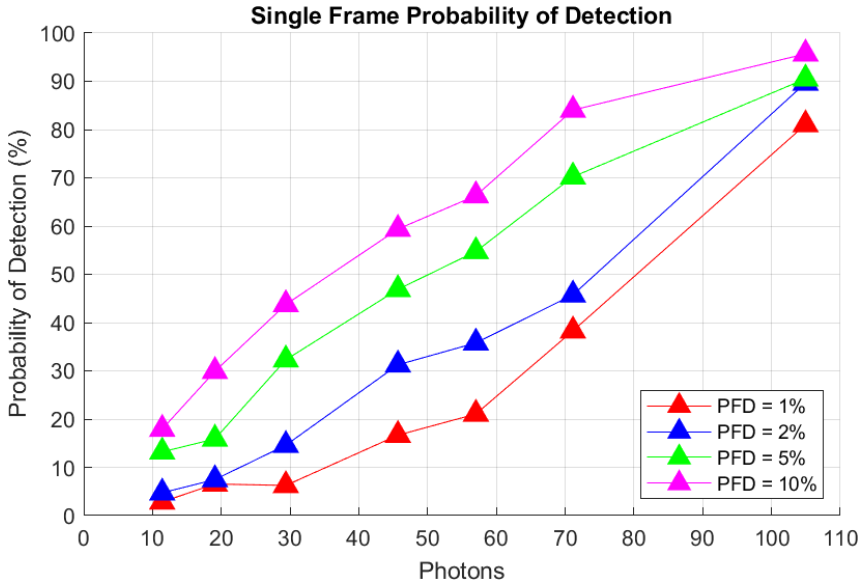

Figure 5: Probability of detection at each photon flux using different variations of the pulse detection algorithm which correspond to different probabilities of false detection.

3.3 Performance with frame summing

Frame summing or frame averaging is a technique used to increase the signal-to-noise ratio by summing or averaging several repeated measurements. The effect of this technique when applied to the raw GSFL data is shown in Figure 6 where each plotted line corresponds to data taken from the individual clusters marked in Figure 4. As the number of averaged frames increases, the pulse shape becomes less noisy and more defined. This not only improves the probability of detection, but will also reduce the noise of the range calculation. Note the pulse shape is different for the 100-photon pulse because the range gate (sample window) is shifted slightly from the other six clusters.

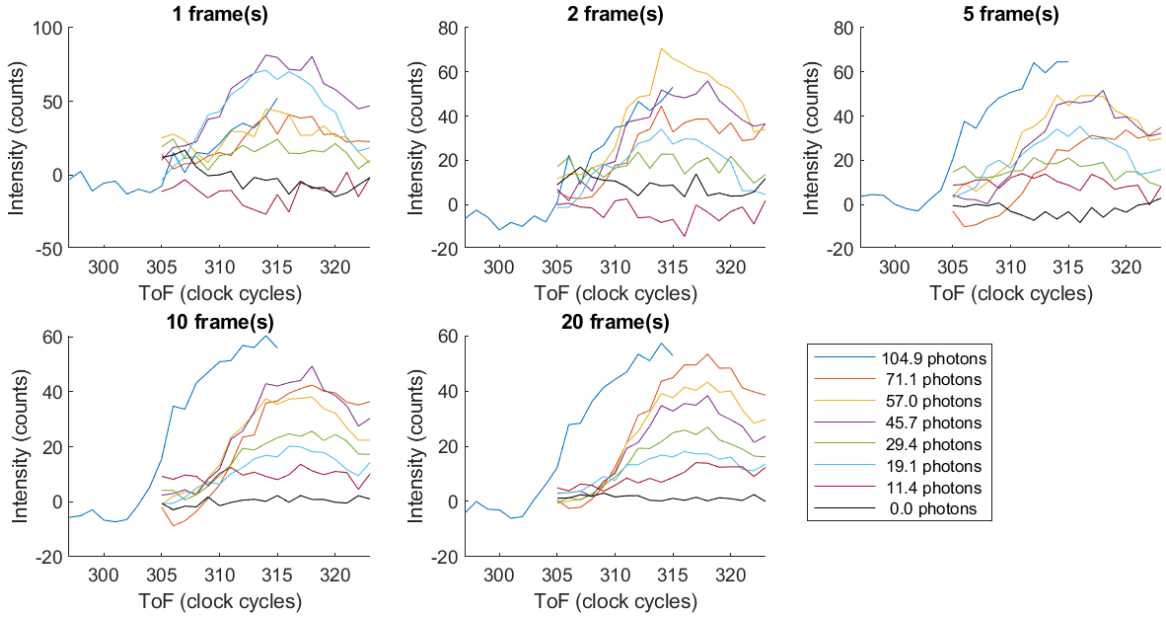

Figure 6: Frame averaging applied to GSFL raw data.

To improve on the PD performance shown in Figure 5, the same pulse detection technique defined in Section 3.2 was applied to the frame averaged data. The resultant PDs are shown in Figure 7 for a variety of frame lengths with the threshold tuned to a PFD of 5%. Like the PFD, the acceptable number of averaged frames is application specific, but these results show with at least 5 frames, a 30-photon pulse is detectable 80% of the time – further improving the detection threshold.

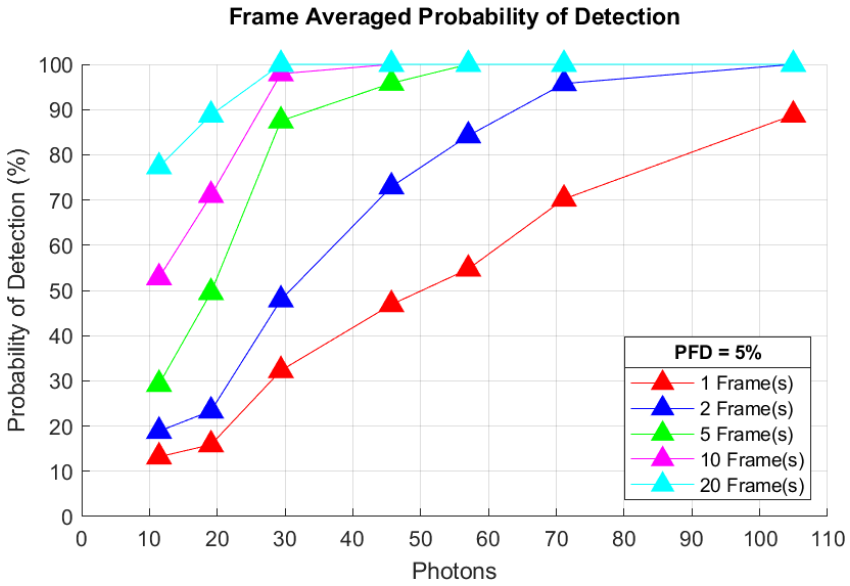

Figure 7: Probability of detection of pulse detection algorithm applied to frame averaged pulse shapes.

4. CONCLUSION

4.1 Future development

With its latest GSFL design, ASC has developed a highly sensitive FPA that utilizes APDs operated in linear mode. These APDs coupled with a low-noise readout that is capable of gated-mode operation give the GSFL sensitivity comparable to Geiger Mode LIDAR. For a single frame, ASC has demonstrated a detection threshold of 100 photons, and with the aid of frame summing, a detection threshold of below 30 photons.

The detection threshold was quantified with a simple pulse detection algorithm that utilizes a matched filter. Going forward, this pulse detection algorithm could be developed further to improve performance for both the single and frame summed cases. For this test, the algorithm was implemented in software and used to post-process raw data collected by the GSFL testbed. This algorithm is not more complicated than the range algorithm already implemented in the onboard FPGA. Therefore, these calculations could be made in real-time while the LIDAR is running at rate.

The data collected for this test was all taken at room temperature (20°-25°C). The GSFL FPA noise decreases as the detectors are cooled and, therefore, cooling the sensor should yield further improvements. One of the next steps is to repeat this experiment with active cooling and determine the trade-off between improved sensitivity and power needed for cooling.

Finally, ASC is working on an improved readout design that can be incorporated with higher sensitivity InGaAs APD detector arrays. Legacy APD arrays have a typical gain multiplication of ~10X. Commercially available array gain multiplication has now improved to >40X. The gain improvements enable readout designs with smaller pixel pitches and higher pixel counts. Also, ASC and Continental have demonstrated readout designs with 128-cell buffers instead of a 20-cell buffer. This readout design is well suited to the high sensitivity applications as the large buffer simplifies and speeds up searching algorithms which can be implemented onboard or in application software.

4.2 Applications

ASC's GSFL has been demonstrated for rendezvous and birthing aboard the Dragon vehicle, landing during NASA's Autonomous Landing and Hazard Avoidance Technologies (ALHAT) project [5], on-orbit testing aboard Endeavor and in deep space operations aboard OSIRIS-REx. The improved FPA sensitivity performance extends the capability of the GSFL for these applications and to other space and terrestrial applications. Specifically, the lower detection threshold allows for a wider FOV and/or extended range performance (>10km). Wide FOV imaging is highly desired for short range automotive applications, satellite proximity operations, and UAV mapping applications. Long range performance is need for space and airborne object detection, identification, and tracking applications.

REFERENCES

[1] Pack, R. T., Brooks, et al., "An Overview of ALS Technology," Ed. Renslow, S., [Manual of Airborne Topographic LIDAR], American Society for Photogrammetry and Remote Sensing, Bethesda, 69 (2012).

[2] Stettner, R., and Bailey, H. W., "3D Imagining Underwater Laser Radar," United States Patent 5446529 (1995).

[3] Stoker, J. M., Abdullah, Q. A., Nayegandhi, A., Winehouse, J., "Evaluation of Single Photon and Geiger Mode Lidar for the 3D Elevation Program," Remote Sens, 8, 767 (2016). https://doi.org/10.3390/rs8090767

[4] Amzajerdian, F., Vanek, M., Petway L., Pierrottet, D., Busch, G., and Bulvshev, A., "Utilization of 3D imagining flash lidar technology for autonomous safe landing on planetary bodies," Proc. SPIE 7608, Quantum Sensing and Nanophotonic Devices VII, 760828 (22 January 2010); https://doi.org/10.1117/12.843324

[5] Roback, V. E., Amzajerdian, F., Bluyshev, A. E., Brewster, P. F., and Barnes, B. W., "3D flash lidar performance in flight testing on the Morpheus autonomous, rocket-propelled lander to a lunar-like hazard field," Proc. SPIE 9832, Laser Radar Technology and Applications XXI, 983209 (13 May 2016); https://doi.org/10.1117/12.2223916